A Theory of Rotating Stall of Multistage Axial Compressors: Part II—Finite Disturbances[1]

F. K. Moore
Sibley School of Mechanical and Aerospace Engineering, Cornell University, Ithaca, N.Y. 14853

A small-disturbance theory of rotating stall in axial compressors is extended to finite amplitude, assuming the compressor characteristic is a parabola over the range of the disturbance. An exact solution is found which requires the operating point to be at the minimum or maximum of the parabola. If the characteristic is flat in a deep-stall regime, the previous harmonic solution applies with neither reverse flow or "unstalling." If the characteristic is concave upward in deep stall, the disturbance has a skewed shape, steeper at the stall-zone trailing edge as experiment shows. Propagation speed is only slightly affected by this nonlinearity. Near stall inception, negative curvature in combination with multiple stall zones can limit the nonlinear oscillation, in the manner of "progressive" stall. If, as seems likely, lag at stall inception is negative (opposite to inertia), propagation speed exceeds 1/2 wheel speed, as experiments suggest.

Introduction

In Part I ("Small Disturbances") [1], it was shown how a combination of three lags, pertaining to entrance-flow passage, compressor blade passage, and exit-flow passage permit the occurrence of a flow distortion which is steady in a moving frame of reference. In principle, the entrance and exit lags are easily calculated, while the blade-passage lag is difficult to define and infer from tests. Comparison with measurements of rotating-stall propagation speed made by Day and Cumpsty [2] support the idea that the blade-passage effect is largely inertial, in deep stall.

The lag per row was represented as a factor, k, of the purely inertial value for a blade passage. If the inter-row gap is equal to the blade depth, then k would be about 2, still considering only inertia but including the mass of fluid occupying the inter-row space. The combined lag effects of entrance and exit flows was represented by the factor, m; if long straight passages describe both entrance and exit configurations, then $m=2$.

For small perturbations, k and m enter as a ratio in the formula for propagation speed. If the ratio is taken as 2 (about twice what we would expect on purely inertial grounds), agreement with experiment is very complete, suggesting that a single compressor lag parameter, if suitably chosen, could lead to a quite complete description of rotating stall.

Small perturbations restrict wave forms to be harmonic, which is quite unlike the wave forms actually observed [2]. Furthermore, the amplitude is unspecified in a linear analysis. Thus, although a good prediction of propagation speed is encouraging, the important questions about rotating stall have to do with disturbances of finite amplitude. Specifically:

1 What is the effect on average pressure-rise performance caused by rotating stall?

2 Are there circumstances which limit the amplitude of oscillation? If so, "progressive stall" may be indicated.

3 Are there ranges of flow coefficient for which rotating stall is forbidden? If so, "stall recovery" may be indicated.

In considering these questions, we should, if possible, allow the assumed compressor characteristic to depart from a constant value during the oscillation of flow coefficient.

In this paper, we investigate the finite-strength disturbances permitted when the characteristic is either flat or has constant curvature. Notation will be as defined in Part I, except for quantities appearing for the first time; these appear in the Nomenclature.

Solutions of the Pressure Equation

The Disturbance Equations. We recall the basic pressure-match equation, equation (36) of Part I, and incorporate equations (37) and (39)

$$\lambda g'(\theta) - mfh + \frac{1}{2}(1-K_I)h^2 + \Psi - \psi_c(c) = 0 \qquad (1)$$

where g and h are the axial and circumferential velocity disturbances, related by the Fourier series (equation (18)) of Part I, or the equivalent statement

$$h + ig = \text{analytic function of } (e^{i\theta}) \qquad (2)$$

[1] Research performed at NASA-Lewis Research Center

Contributed by the Gas Turbine Division of THE AMERICAN SOCIETY OF MECHANICAL ENGINEERS and presented at the 28th International Gas Turbine Conference and Exhibit, Phoenix, Arizona, March 27-31, 1983. Manuscript received at ASME Headquarters December 20, 1982. Paper No. 83-GT-45.

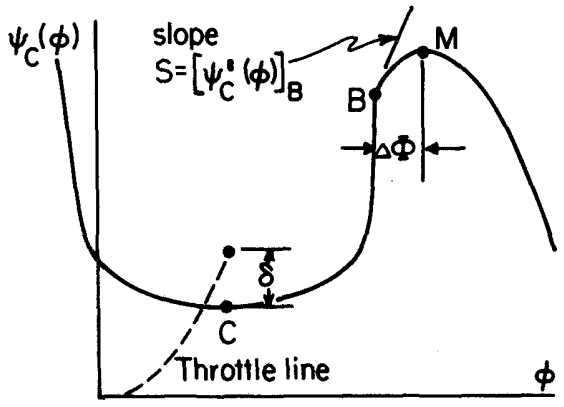

Fig. 1 Constant-speed compressor characteristic in the absence of rotating stall

We will assume that the rotating stall-free characteristic function remains well represented, over the range of the oscillation, by the first three terms of a Taylor series (equation (38) of Part I) about the mean flow Φ

$$\psi_c(\phi)=\psi_c(\Phi)+\psi_c'(\Phi)g+\frac{1}{2}\psi_c''(\Phi)g^2+\ldots \tag{3}$$

We will find that no solutions are possible unless $\psi_c'(\Phi)=0$, even for finite disturbances. Such a term would represent a damping effect, even for finite disturbances, and must be discarded if only the three terms of equation (3) are considered. The reasons why this is true will be made clear later, especially in Part III.

Equation (1) now becomes

$$\lambda g'(\theta)-mfh+\frac{1}{2}(1-K_I)h^2-\frac{1}{2}\psi_c''(\Phi)g^2+\delta=0 \tag{4}$$

where δ is the performance increase (perhaps negative) due to rotating stall

$$\delta\equiv\Psi-\psi_c(\Phi) \tag{5}$$

A typical function $\psi_c(\Phi)$ and positive δ are sketched in Fig. 1.

The second term of equation (4) embodies the factor m, introduced in Part I to account for lags external to the compressor. This factor was found to be 2 for small disturbances of a straight-channel exit. In the present paper, we are concerned with finite disturbances, and a more complete accounting for downstream pressure recovery is no doubt needed. The necessary analysis would be very arduous and not justified for a particular highly idealized exit channel. For a sudden exit expansion, we argued that $m=1$, and this result is independent of amplitude. Therefore, the term mfh will be retained because it is proper when $m=1$, and may be empirically justified for other values of m. Further research on this point is required.

The disturbances, g and h, governed by equation (4) are periodic (but not necessarily harmonic) and have vanishing averages over a cycle: in the case of g because it is defined as a departure from average axial velocity, and in the case of h, because net circulation in the entrance flow is assumed to remain zero. Therefore, integrating equation (4) over a cycle shows that, when nonlinear terms involving h^2 and g^2 are included, the constant δ cannot be zero, as it was in the linear analysis of Part I.

A General Solution. In Part I, equations (2) and (4) had a simple harmonic solution because the last three terms of equation (4) were absent. Here, those terms are kept, and appropriate nonlinear periodic solutions are sought. It happens that a general solution, believed to be unique, can be written down at once

$$h+ig=A\frac{e^{in\theta}}{1+\eta e^{in\theta}} \tag{6a}$$

or

$$h=\frac{A(\cos n\theta+\eta)}{1+\eta^2+2\eta\cos n\theta};\quad g=\frac{A\sin n\theta}{1+\eta^2+2\eta\cos n\theta} \tag{6b}$$

where A and η are constants to be determined by satisfying equation (4). In order that h and g have Fourier series in θ of the form of equations (18) of Part I, it is necessary that $|\eta|<1$. Equation (6a) is clearly a special case of equation (2), and the previous linear solution is recovered by setting $\eta=0$.

The forms of these velocity traces are shown for various values of η between 0 and 1, on Fig. 2. The axial-flow disturbance, g, is antisymmetric and is traveling to the right. Its negative portion represents a "stall zone"; if A is positive, its "trailing edge" is steeper.

In presenting the results for A and η obtained by substitution into equation (4), we note that f is not known and recall that

$$\lambda=\frac{2UN\tau}{D}\left(\frac{1}{2}-f\right)-\frac{2U\tau_v}{D}f \tag{7}$$

if the lags for IGV and OGV are equal. Thus, a free constant will remain after η, A, and δ are given in terms of f. Results are

$$\frac{\lambda n}{mf}=\frac{(1-\eta^2)\psi_c''+(1-5\eta^2)(1-K_I)}{(1+\eta^2)\psi_c''+(1-3\eta^2)(1-K_I)} \tag{8}$$

$$A=\frac{4mf\eta}{\psi_c''}\frac{(1-\eta^2)\psi_c''+(1-3\eta^2)(1-K_I)}{(1+\eta^2)\psi_c''+(1-3\eta^2)(1-K_I)} \tag{9}$$

$$\delta=\frac{Amf}{8\eta^2}[4\eta-Amf(\psi_c''+1-K_I)] \tag{10}$$

The next step will describe rotating-stall features implied by

Nomenclature

A = amplitude coefficient of disturbance, equation (6a)
A_1, A_2 = stream-tube areas at entrance to IGV, Fig. 3
a = dimensionless reciprocal time lag, $D/(2UNt)$
B = denotes "break" of characteristic, Fig. 1
C = denotes minimum of deep-stall characteristic, Fig. 1
C_p = disturbance of static-pressure rise coefficient across the compressor, equation (18)
M = denotes maximum of characteristic at stall inception, Fig. 1
S = slope of characteristic at "break point," B, Fig. 1
Δp = pressure recovery at entrance to IGV, equation (11)
$\Delta\Phi$ = difference of flow coefficient at points, M and B, of Fig. 1
η = nonlinearity parameter of disturbance, equation (6a)
δ = performance increase due to rotating stall, equation (5)

Subscripts

m = amplitude of axial velocity disturbance
mm = conditions when axial velocity disturbance amplitude has its largest permitted value

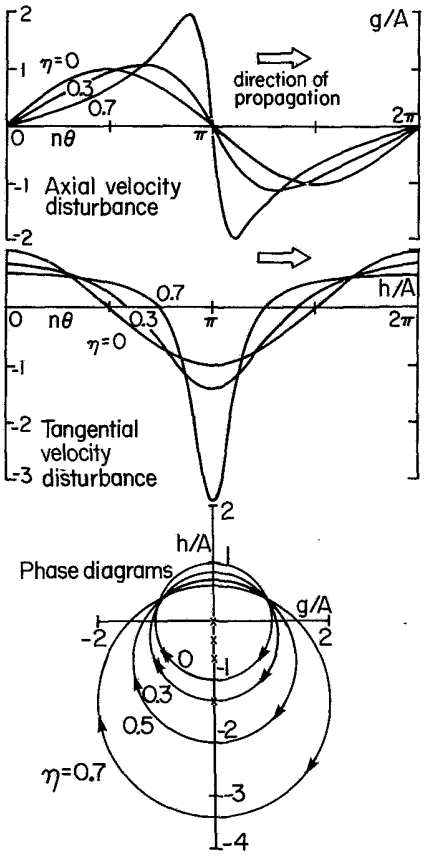

Fig. 2 Nonlinear velocity disturbances, for various values of amplitude parameter η, from equations 6(*a*) and 6(*b*)

equations (8–10). First, we should specify the parameters $\psi_c''(\Phi)$ and K_I.

In these equations, K_I is the coefficient of pressure recovery in the entrance of the IGV passage, owing to the fact that a transverse velocity disturbance makes an incoming stream tube somewhat narrower than the IGV entrance. Figure 3 sketches the process. The conservative estimate of this effect is gotten by assuming the area increase is sudden. The usual pressure-rise formula in such a case is

$$\frac{\Delta p}{\rho(V^2+u^2)} = \frac{A_1}{A_2}\left(1-\frac{A_1}{A_2}\right)$$

but the geometry of Fig. 3 shows that $A_1/A_2 = V/\sqrt{V^2+u^2}$. Since $V = U\phi$ and $u = Uh$ in stator coordinates, we may conclude that

$$\frac{\Delta p}{\rho U^2} = \phi^2[\sqrt{1+(h/\phi)^2}-1] = \frac{1}{2}h^2K_I \tag{11}$$

the last member of the equation being the definition of K_I. The quantity $1-K_I$ which appears in equations (8–10) is the head loss coefficient due to oblique entrance to the IGV. Clearly, it is a function of h itself, and therefore cannot properly be used in equation (4) as a constant. Fortunately, the magnitude of $1\text{-}K_I$ is very small, not exceeding 10 percent unless h/ϕ exceeds 0.7. Therefore, one is probably justified in neglecting the head-loss effect represented by $1-K_I$, and equations (8–10) become

$$\frac{\lambda n}{mf} = \frac{1-\eta^2}{1+\eta^2} \tag{12}$$

$$A = \frac{4mf}{\psi_c''}\frac{\eta(1-\eta^2)}{1+\eta^2} \tag{13}$$

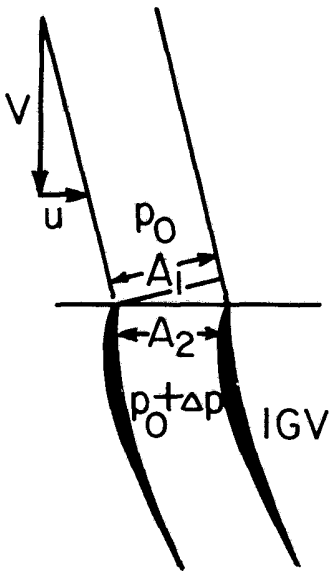

Fig. 3 Sketch of the increase of stream-tube area from A_1 to A_2 upon entry into an IGV passage, owing to transverse disturbance velocity, *u*

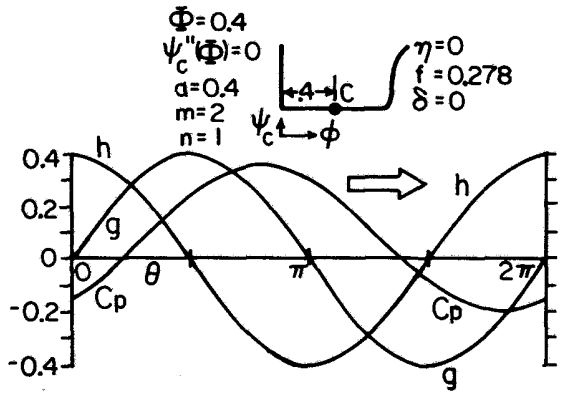

Fig. 4 Velocity and pressure disturbances for a flat characteristic ($\psi_c''(\Phi)=0$) in deep stall. Stall zone is $180 < \theta < 360$ deg, where $g < 0$.

$$\delta = \frac{4(mf)^2}{\psi_c''}\frac{\eta^2(1-\eta^2)}{(1+\eta^2)^2} \tag{14}$$

We bear in mind that λ is a given function of f (equation (7)), and therefore equation (12) is an equation connecting f and η. In fact, equation (12) may be replaced by

$$f = \frac{1/2}{1+\dfrac{\tau_v/\tau}{N}+\dfrac{am}{n}\dfrac{1-\eta^2}{1+\eta^2}} \tag{15}$$

where the symbol a is introduced to define the group

$$a \equiv \frac{D}{2UN\tau} = \frac{D}{NL}\frac{\Phi}{2\tau^*} \tag{16}$$

and the last expression results from equation (45) of Part I. In discussing compressors of many stages, one might well neglect the second term of the denominator of equation (15), finding

$$f = \frac{1/2}{1+\dfrac{am}{n}\dfrac{1-\eta^2}{1+\eta^2}} \tag{17}$$

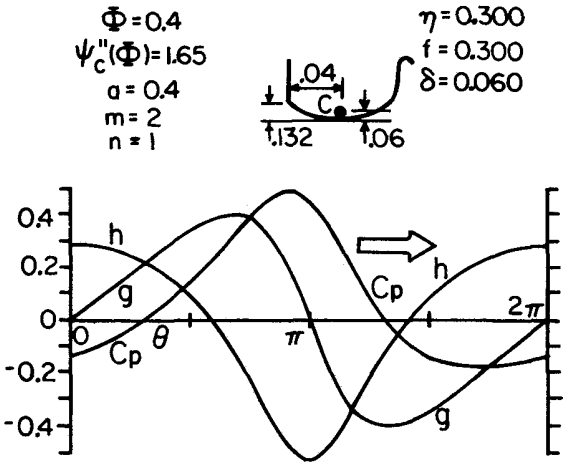

Fig. 5 Velocity and pressure disturbances for a concave characteristic ($\psi_c''(\Phi) > 0$) in deep stall. Stall zone is $180 < \theta < 360$ deg, where $g < 0$.

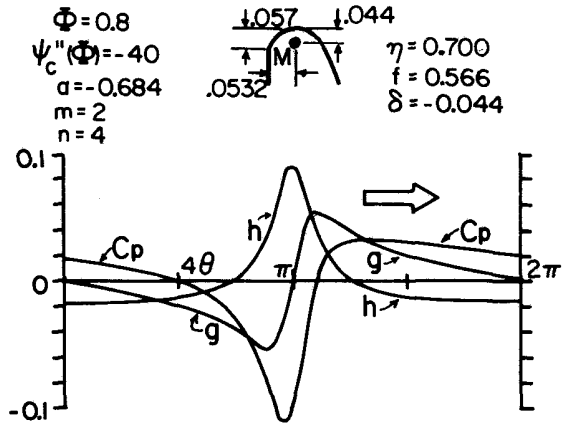

Fig. 6 Velocity and pressure disturbances for a convex characteristic ($\psi_c''(\Phi) < 0$) at incipient stall (note expanded scales). Stall zone is $0 < 4\theta < 180$ deg, where $g < 0$.

Pressure Disturbance. We should record for subsequent use an expression for pressure-rise fluctuation, because that is a quantity more easily measured than the velocity components represented by g and h. Equations (8) and (9) of Part I and the present equations (4) and (5), with $K_I = 1$, yield the static pressure rise across the compressor

$$C_p \equiv \frac{p_e - p_0}{\rho U^2} - \left[\frac{1}{2}\Phi^2 + \Psi(\Phi)\right] = -mfh + \Phi g + \frac{1}{2}g^2 + \frac{1}{2}h^2 \tag{18}$$

Included in brackets on the left of this equation are certain quantities which will be constant during any rotating-stall process. Quantities which will fluctuate are on the right side, and they are the ones of most interest.

Amplitude of Solution. We have noted that equation (6*b*) describes an oscillation of axial flow (g) that is symmetrical: its amplitude can be found using equations (13) and (17) to be

$$g_m = \frac{2m}{\psi_c''} \frac{\eta}{\left(1+\frac{am}{n}\right)+\eta^2\left(1-\frac{am}{n}\right)} \tag{19}$$

with η being an amplitude parameter as yet undetermined.

As a function of η, the disturbance amplitude, g_m, might be limited in some circumstances. According to equation (19), the maximum value that g_m can assume is

$$g_{mm} = \frac{m}{\psi_c''} \frac{1}{\sqrt{1-(am/n)^2}} \tag{20}$$

when

$$\eta_{mm} = \sqrt{\frac{1-(am/n)}{1+(am/n)}} \tag{21}$$

In such a case, equations (17) and (14) give

$$f_{mm} = \frac{1/2}{1-(am/n)^2}; \quad \delta_{mm} = -\frac{m^2}{\psi_c''} \frac{am/n}{[1-(am/n)^2]} \tag{22}$$

Because η is restricted to be less than 1, equation (21) shows that this particular limiting solution is possible only if a is negative, and that requires τ to be negative; in effect, the hysteresis loop of Fig. 3 of Part I would be clockwise in such a case.

If, on the other hand, a is positive, equation (19) shows that maximum would occur when $\eta = 1$, taking the value $g_{mm} = m/\psi_c''$.

Next, we should apply these results for interesting choices of ψ_c'', indicated on Fig. 1. There are two types of points where the characteristic (in absence of rotating stall) is horizontal ($\psi_c''(\Phi) = 0$) but yet has nonzero curvature. They are indicated on Fig. 1 as points C and M. At point C, the curvature $\psi_c''(\Phi)$ is positive, while at M it is negative.

Deep Stall

Flat Characteristic. At a point such as C of Fig. 1, we first consider the possibility that $\psi_c'' = 0$ everywhere in the range of oscillation. In that case, equation (19) shows that η must be zero if g_m is to be finite, and equations (17) and (14) give

$$f = \frac{1/2}{1+(am/n)}; \quad \delta = 0 \tag{23}$$

This is simply the harmonic solution discussed in Part I, with, according to equation (6*b*),

$$h = g_m \cos n\theta; \quad g = g_m \sin n\theta$$

We conclude that in a region where the characteristic is flat, the solution is the linear one with arbitrary amplitude, even though a nonlinear solution is allowed. This result perhaps explains the surprising outcome of Part I, that a small-perturbation theory yields a good representation of stall propagation speed, even though the actual stall amplitude is large. For realistic comparison with experiment, the lag τ, and hence a, is positive, corresponding to values of $f < 1/2$.

The amplitude cannot actually be unlimited, of course. We suppose that this linear solution will be appropriate for rather small mean flow coefficients, so that the oscillation does not intrude into the rising part of the characteristic, with "unstalling" becoming a feature of the oscillation. In the same way, we would forbid the flow to reverse, imagining an abrupt rise of the characteristic below $\phi = 0$. If this is true, the oscillation should have an amplitude limited by Φ itself. That is

$$h = \Phi \cos n\theta; \quad g = \Phi \sin n\theta \tag{24}$$

Although the velocity components are harmonic, the pressure fluctuation is not, according to equation (18): If $n = 1$

$$C_p = \frac{1}{4}\Phi^2 - mf\Phi\cos\theta + \Phi^2\sin\theta \tag{25}$$

If, for example, $\Phi = 0.4$, $a = 0.4$, and $m = 2$, the velocity and pressure-rise fluctuations would be shown in Fig. 4. The pressure trace is also harmonic. The propagation is toward the right of the figure, at a speed (f) of 0.278. In this case, of course, $\delta = 0$, because $\eta = 0$. The operating point lies at point C, on the characteristic, as indicated in the sketch.

Concave Characteristic. Next we consider the possibility that $\psi_c'(\Phi)$ is slightly positive, or concave, as at point C of Fig. 1. Again, we expect that a is positive (on the ground that deep stall seems always to have $f < 1/2$). In that case, the greatest possible value of η would be 1, but then only if ψ_c'' is larger than m/g_m according to equation (19). For realistic diagram shapes, ψ_c'' must be much less than m/Φ, and we therefore conclude that η is quite small in these cases.

From equation (19), setting $g_m = \Phi$ and making η small gives

$$\eta = \frac{\psi_c''}{2m}\left(1 + \frac{am}{n}\right) \tag{26}$$

Substitution of equation (26) into previous equations will give corrections of order ψ_c'' to the flat-characteristic solutions. While the predicted traces of g and h as well as δ, will change to first order in ψ_c'', the value of f will be affected only to second order.

If $\psi_c'' > 0$, then A is positive and the velocity traces are as in Fig. 2, with an axial flow disturbance (g) which is steepest at the stall-zone "trailing edge," as experiments have shown [2]. By way of example, we modify the example displayed in Fig. 4, by making $\psi_c''(\Phi) = 1.65$; the changed characteristic is sketched in Fig. 5. Equation (18) gives the corresponding pressure trace, C_p. Pressure rise as well as axial velocity demonstrate the steep "trailing edge" found experimentally.

Incipient Stall

Convex Characteristic. At a point such as M, the value of ψ_c'' is negative. At a given speed, as flow coefficient, Φ, is reduced, rotating stall can first appear at point M. The characteristic of Fig. 1 is drawn to show some degree of overturn to the left of M, terminated in an abrupt drop at point B. At that point, we imagine a certain positive slope, S, to occur. The final slope, S, depends on the compressor; lightly-loaded compressors tend to permit a large S before a steep break occurs. If a parabola is used to represent the curve in the stall-inception zone, centered on point M, one could relate S to ψ_c'' and the distance, $\Delta\Phi$, between points B and M on the diagram

$$\Delta\Phi = S/\psi_c'' \tag{27}$$

As we have seen, a stall oscillation about point M would have a maximum permissible amplitude g_{mm} depending on the sign of τ (or a)

$$\left.\begin{aligned} g_{mm} &= \frac{m/\psi_c''}{\sqrt{1-(am/n)^2}}, \quad a<0 \\ &= m/\psi_c'', \quad a>0 \end{aligned}\right\} \tag{28}$$

If this maximum amplitude exceeds the $\Delta\Phi$ between points B and M, then the oscillation could easily extend into the deep stall zone, and a different type of larger amplitude oscillation would result, of the sort to be discussed in Part III of this series. On the other hand, if $g_{mm} < \Delta\Phi$, the oscillation could be limited to the vicinity of point M, governed purely by the local convex parabolic segment. This latter situation would presumably relate to "progressive" stall.

Because $\psi_c''(\Phi) < 0$, equation (13) shows that $A < 0$. Thus, the trace of g in Fig. 2 is reversed in sign, and now it is the cell "leading edge" that is the steeper. The proper value of η can be found from equation (19), if g_m is fixed.

Progressive Stall. Pursuing this idea further, we can relate g_{mm} and $\Delta\Phi$ from equations (27), (28) to arrive at the criteria for limited, or progressive-type stall

$$S > \frac{m}{\sqrt{1-(am/n)^2}}, \quad a<0 \tag{29}$$

$$S > m, \quad a>0 \tag{30}$$

These equations indicate that progressive stall is favored if:

1 S is large. Experience confirms that a delayed "break," and hence large S, favors progressive stall.

2 m is small. That is, an abrupt expansion at exit as opposed to a long, straight discharge would favor progressive stall. It is not known whether experience confirms this prediction.

3 n is large, if $a < 0$ (clockwise hysteresis). Large n denotes many stall cells, and experience is quite definite that progressive stall is associated with multiple stall cells [2]. We find that n is relevant only if $a < 0$ and, therefore, $f > 1/2$ (equation (22)). It is also usually found that progressive stall has this feature as well (see [2] or Table 1 of Part I), and we conclude that clockwise hysteresis ($a < 0$, $\tau < 0$) is quite typical in these "soft-stall" cases. Theoretically, it has been argued [3] that lift hysteresis of a single airfoil is of this sense if its stall process is a progressive advance of trailing-edge separation as opposed to the more abrupt leading-edge stall. In the former case, lift curves are rounded, while in the latter case, an abrupt break occurs. Thus, there is some basis for expecting $\tau < 0$ for progressive compressor stall.

4 a is small, if $a < 0$. Actually, am and n should be considered together; equation (17) provides

$$\frac{am}{n} = \frac{Dm}{2UNn\tau} \tag{31}$$

This grouping suggests that large τ favors progressive stall, as does a large product Nn. Perhaps it may be inferred that large n is especially required for single-stage ($N = 1$) progressive stall, whereas multistage machines can have progressive stall which does not split up into multiple cells, because Nn is large even if $n = 1$. Experimental results tend to support this idea.

Figure 6 shows velocity and pressure-rise fluctuations calculated for a limited oscillation of the sort just discussed with a negative and ψ_c'' quite large and negative, n was taken to be 4, and the stall point M was considered to occur at $\Phi = 0.8$. The amplitude is only 0.053, but η is quite large because ψ_c'' is large, and the traces are quite far from harmonic shape. Propagation speed is greater than 1/2, and axial velocity changes most rapidly at the cell leading edge, in contrast to the case when $\psi_c'' > 0$. This result is in contrast to the known tendency of deep-stall wave forms to be steeper at the cell trailing edge [4]. Probably, the differing curvatures of ψ_c are important in this regard. Perhaps it would be useful to investigate this aspect of progressive stall experimentally.

Limitations of the Analysis. Multicell progressive stall is usually also part-span stall [2]. The present analysis assumes two-dimensional flow; in effect, full-span disturbances are assumed. The importance of this inconsistency with observations is difficult to assess.

The foregoing analysis does not show that rotating-stall oscillations must extend to the allowed amplitude limits, or that the oscillation will choose, so to speak, to adopt a zone number appropriate to progressive stall. Neither is it shown that the oscillation will become of the large-amplitude type just because it is not limited to remain above point B. These questions are ones for future research, probably to be answered by studying limit cycles emerging from equation (4). The present analysis is intended to suggest features to look for, in those more complete and inevitably more complex and confusing solutions.

Finally, we should recall the criterion $\psi_c'(\Phi) = 0$, mentioned following equation (3). Of course, a throttle setting need not correspond to $\Phi'(\Phi) = 0$. However, a purely periodic wave cannot occur, governed by a purely parabolic characteristic

unless that is true, even if the motion is nonlinear. The reason for this result, which will be made clear in Part III, is essentially that mentioned in Part I; namely, that $\psi_c'(\Phi)$ would be an amplification coefficient in equation (3). If $\psi_c'(\Phi)=0$, then any oscillation would grow until it encountered new features of the function $\psi_c(\Phi)$, beyond the range of the assumed parabola, such as a resistance to reversed flow, and this encounter would lead finally to a limit cycle. If $\psi_c'(\Phi) < 0$, then the oscillation would presumably disappear by damping.

Thus, if Φ is intermediate between points B and M, rather than at M, an oscillation would presumably amplify to include some involvement with the steep drop at B. This case is beyond the scope of this paper.

Concluding Remarks

Finite-amplitude rotating stall has been analyzed for cases in which it may be assumed that the constant-speed characteristic is parabolic in flow coefficient with rotating stall absent. It was found that a periodic solution (neither damped nor amplified) requires a horizontal slope of that characteristic at the given average flow. Presumably, if the slope were negative, the oscillation would be damped, but if it were positive, the oscillation would grow until new features of the characteristic curve (reverse flow or stall recovery) become influential.

In "deep stall," if the characteristic is flat, the solution differs only slightly from the linear one, perhaps explaining why propagation speeds from Part I agree so well with experiment. In this case (Figs. 4 and 5), the oscillation would presumably be limited by reverse-flow resistance, provided flow coefficient is quite low (less than half the coefficient at stall). At larger flow coefficients, even if the characteristic is locally flat, interaction with the unstalled part of the characteristic will occur, and the resulting motion will become nonharmonic on that account. This is the subject of Part III of this series.

The characteristic function $\psi_c(\phi)$ we have used is artificial in the sense that it is defined in the absence of rotating stall, and therefore is not normally measured in compressor tests. However, it is perfectly well defined physically, and could be measured in experiments designed to suppress rotating stall. It is defined for the compressor alone, and therefore one is free to manipulate exit and entrance conditions in order to prevent rotating stall, and also to eliminate any irrelevant hysteresis effects of a control throttle.

In incipient stall conditions, the stall oscillation may be limited in amplitude by a strong reverse curvature of the characteristic, permitting a progressive type of stall. If the characteristic "turns over," so that the break of the speed line is delayed substantially below maximum pressure rise, then this limited solution is favored. If the force lag is negative (opposite in sense to the effect of inertia) then two notable results appear: the propagation speed exceeds $1/2\ U$, and the limited-amplitude solution is favored for multiple cells. Because experiments usually show these same features, the inference seems warranted that lag (τ) is indeed negative in the incipient or progressive stall region.

In the deep-stall region, nonlinearity associated with concave curvature of the characteristic provides a steepening of the stall-zone trailing edge, as experiments show, provided lag (τ) is positive. Probably, then, lag should be taken positive in deep stall, and negative in incipient stall. Experiments are needed to establish these blade-passage lags.

Theory and experiment are both needed to describe the entrance and exit flows, especially for the relation between axial and transverse velocity disturbances. The present theory shows that rotating stall is sensitive to these conditions (lumped, in the present theory, in the parameter, m), and practical control means could well evolve from such a study.

A new type of experiment is needed to find the compressor characteristic in the absence of rotating stall, and free of irrelevant throttle hysteresis. Experiments have suggested that exhaust to low pressure through a high-resistance screen may suppress rotating stall even at fully stalled flow rates, and also that unwanted throttle effects can be eliminated by lowering pressure behind the throttle (see [4], Fig. 19). Therefore, it seems feasible in principle to measure $\psi_c(\phi)$.

The present theory shows that the characteristics with and without rotating stall are different (δ represents that difference) and thus that rotating stall affects average compressor performance. Ultimately one can envisage a theory in which surge and rotating stall are integrated, rather than being considered separate and independent phenomena. One would then be able to deal with engine dynamics on a fundamental basis.

A nonlinear, unsteady model of rotating stall has been presented by Takata and Nagano [5] for single rows and pairs of rows; in it they permit the upstream potential flow and downstream vortical flow to be unsteady and make the required calculations numerically. One of their equations can be specialized for steady disturbances and purely inertial compressor lag to give the first two terms of equation (1) with $m = 1$ (constant exit pressure). Their treatment of blade-row losses and pressure rise is quite different from that used here, and seems quite unsuitable for multistage compressors. Their chief concern was to analyze the growth of initially weak disturbances into rotating stall of single rows and stages.

In the next and concluding paper of this series, oscillations will be allowed to interact with the entire characteristic diagram, so that resistance to reverse flow and "unstalling" affect the disturbance pattern.

References

1 Moore, F. K., "A Theory of Rotating Stall of Multistage Axial Compressors: Part I — Small Disturbances," ASME Paper No. 83-GT-44, 28th International Gas Turbine Conference, Mar. 1983, pp. 313–320.

2 Day, I. J., and Cumpsty, N. A., "The Measurement and Interpretation of Flow within Rotating Stall Cells in Axial Compressors." *Journal of Mechanical Engineering Sciences*, Vol. 20, 1978, pp. 101–114.

3 Moore, F. K., "Lift Hysteresis at Stall as an Unsteady Boundary-Layer Phenomenon," NACA TN 3571, 1955. Also, Hartunian, R. A., "Research on Rotating Stall in Axial-flow Compressors. Part I. On Lift Hysteresis at Maximum Lift Including Effect of Camber," WADC TR 59-75, Jan. 1959.

4 Day, I. J., Greitzer, E. M., and Cumpsty, N. A., Stall," ASME JOURNAL OF ENGINEERING FOR POWER, Vol. 100, Jan. 1978, pp. 1–14.

5 Takata, H., and Nagano, S., "Nonlinear Analysis of Rotating Stall," ASME JOURNAL OF ENGINEERING FOR POWER, Oct. 1972, pp. 279–293.